GEOPHYSICS, VOL. 69, NO. 5 (SEPTEMBER-OCTOBER 2004); P. 1272–1282, 7 FIGS., 3 TABLES.
10.1190/1.1801944

The optimization approach to lithological tomography: Combining seismic data and petrophysics for porosity prediction

Miguel Bosch[1]

ABSTRACT

Least-squares model optimization methods are commonly used to estimate physical media properties by fitting geophysical data with nonlinear models. I extend this formulation to joint estimation of physical properties and lithological description of the media. Incorporation of petrophysical information within the inversion scheme provides the coupling between lithology and media physics by describing the geostatistical relation between them. The resulting procedure adjusts iteratively the joint model to simultaneously fit geophysical data, the petrophysical statistical medium description, and prior information on the lithology, following equations derived for the Newton's optimization method. Although more calculations are required to incorporate the additional information and estimate the model update, the algebraic system of linearized equations can be transformed appropriately to remain within the same dimensions of the conventional inverse formulation. In the particular case when the petrophysical transform is linear (i.e., the function of lithological parameters that provides the expected values of the physical parameters), the lithological inversion equations are equivalent to the corresponding equations of a conventional inversion followed with the inverse petrophysical transform. I illustrate the methodology with synthetic examples of porosity-impedance estimation from zero offset seismic data, using Wyllie's transform to construct the statistical relationship between porosity and impedance. When the porosity range of the test models is on the nonlinear part of the petrophysical transform, the lithological inversion performs significantly better than the conventional inversion. When the porosity range is on an almost linear part of the transform, the performances are equivalent for both approaches.

INTRODUCTION

The objective of geophysical exploration is the inference of media structure and lithology, using physical phenomena to "illuminate" the underground media. In this manner, geophysical techniques provide valuable information to be combined with information from geology, petrophysics, and other earth sciences specialties, the correct integration across disciplines being a key aspect in the technical success of exploration projects.

The importance of integration is commonly emphasized in many activities related to exploration, such as interpretation, data management, and visualization. However, inversion methods in geophysics do not exploit the multidisciplinary character of the information generated in exploration projects. The common inversion approach explains geophysical data with a model based only on physics. I propose extending this approach to explain multidisciplinary data from a joint lithology-structure-physics model. This work focuses on the formulation of inverse problems techniques incorporating within the earth model medium properties indirectly related to geophysical observations (such as lithology indicators, porosity, or composition) and estimating them from the data.

Benefits of such an integrated approach are multifold. Geophysical phenomena, in particular seismic wave propagation, have significant nonlinear dependence on media properties, and the data distribution is spatially restricted. The incorporation of complementary information from petrophysics, or geology, is crucial to focus geophysical data inversion in the realistic region of the model space. It reduces the region of search, helping convergence, reliability, and precision of the estimation. On the other hand, geophysical data constraints on a joint lithological-structural-physical model directly produce estimations of the lithology and structure, which are of major interest.

A general formulation of the lithological inversion problem under a Monte Carlo approach has been described by Bosch (1999). In this work, lithological inversion from geophysical data was formulated for a categorical description of the

Manuscript received by the Editor March 22, 2002; revised manuscript received March 17, 2004.
[1]Formerly Bullard Laboratories, University of Cambridge, Department of Earth Sciences, United Kingdom; presently Universidad Central de Venezuela, Department of Applied Physics, Caracas, Venezuela. E-mail: mbosch@reacciun.ve.

lithology (rock types) and solved using sampling (Monte Carlo) techniques. Applications of this technique have been shown in work by Bosch et al. (2001) and Bosch and McGaughey (2001) using gravity and magnetic data. Similarly, Monte Carlo methods have been used to incorporate petrophysical information (Mosegaard et al., 1997; Torres-Verdín et al., 1999) in seismic data inversion.

However, Monte Carlo methods require relatively fast computations in order to solve the forward problem a large number of times. To perform inversions that demand large computations in the solution of the forward problem (as it is the case for seismic and electromagnetic wave propagation), optimization approaches are convenient. The present work describes the solution of the lithological inversion problem following an optimization approach. The objective is to provide the appropriate linearized system of equations for the model update, both for the physical and for the lithological model components. Additionally, the formulation of this method for continuous parameters describing the lithology allows the explicit incorporation of information on properties such as porosity, lithology indicators, or composition within the model and their estimation from the constraints provided by the geophysical data.

THE LITHOLOGICAL INVERSION PROBLEM

Because this is a problem of combining information, the framework of statistical inference is convenient for this formulation. To describe the information, I use probability density functions defined over the model and data parameter spaces. The posterior probability density describes the result of combining prior and data information (see Tarantola, 1987):

$$\sigma(\mathbf{m}) = cL(\mathbf{m})\rho(\mathbf{m}), \tag{1}$$

with $\sigma(\mathbf{m})$ being the posterior density, $\rho(\mathbf{m})$ the prior density, $L(\mathbf{m})$ the likelihood function, c a normalization constant, and $\mathbf{m}$ the array of model parameters. A list of mathematical symbols used along this work is shown in Table 1.

In the present formulation, the model parameters are a composite, $\mathbf{m} = \{\mathbf{m}_{\text{phys}}, \mathbf{m}_{\text{geo}}\}$, describing a lithological-physical model of the earth media. The first component are model parameters for description of the physical property field (i.e., elastic parameters, mass density, magnetic parameters, or other appropriate according to the geophysical method used). The second component are model parameters for description of lithology and/or structure in a wide sense, which are indirectly involved in the physical response of the media. Examples are lithology indicators, mineral composition, porosity, or other parameters relevant to the exploration target and area, and additionally being significantly related with the physical behavior of the media. Figure 1 illustrates components of the problem in this integrated approach.

Under the combined model space, the joint prior probability can be calculated by the formula of conditional probabilities, $\rho(\mathbf{m}) = \pi(\mathbf{m}_{\text{phys}}|\mathbf{m}_{\text{geo}})\rho_{\text{geo}}(\mathbf{m}_{\text{geo}})$, the first factor being the conditional probability describing dependency of the physical parameters from lithological parameters, and the second factor being the probability density describing the prior information on the lithological parameters. The geophysical likelihood function depends only on the medium parameters directly related to the calculated geophysical data (i.e., explicit in physical law formulation), $L(\mathbf{m}) = L(\mathbf{m}_{\text{phys}})$. Hence, the posterior density, expression 1, takes the form

$$\sigma(\mathbf{m}_{\text{phys}}, \mathbf{m}_{\text{geo}}) = c \underbrace{L(\mathbf{m}_{\text{phys}})}_{\text{geophysics}} \pi \underbrace{(\mathbf{m}_{\text{phys}}|\,\mathbf{m}_{\text{geo}})}_{\text{petrophysics}} \underbrace{\rho_{\text{geo}}(\mathbf{m}_{\text{geo}})}_{\text{geology}}. \tag{2}$$

See Bosch (1999) for extended discussion of the equation 2.

A distance in the lithological model space can be defined with $\mathbf{m}_{\text{geo}}$ being continuous parameters. This makes a difference in

Table 1. Basic symbols used to formulate the lithological inversion method.

Symbol	Description
$\mathbf{m}_{\text{phys}}$	Physical model parameter array
$\mathbf{m}_{\text{geo}}$	Lithological model parameter array
$\mathbf{m}_{\text{geo prior}}$	Prior lithological model
$\mathbf{m}$	Joint model parameter array
$\mathbf{d}_{\text{obs}}$	Observed geophysical data
$\mathbf{d}_{\text{calc}}$	Calculated data
$\sigma(\mathbf{m}_{\text{phys}}, \mathbf{m}_{\text{geo}})$	The joint posterior probability density
$\rho(\mathbf{m}_{\text{geo}})$	The prior probability density on the lithological field
$\pi(\mathbf{m}_{\text{phys}}\|\mathbf{m}_{\text{geo}})$	The probability density of the physical property field conditioned by the lithological field
$L(\mathbf{m}_{\text{phys}})$	The geophysical likelihood function
c, c_1, c_2	Normalization constants
$\mathbf{g}(\mathbf{m}_{\text{phys}})$	Function solving the geophysical forward problem
$\mathbf{f}(\mathbf{m}_{\text{geo}})$	Function providing the mean model physical parameters conditioned by the model lithological parameters
S	The half sum of squares (objective function)
$\mathbf{G}$	The gradient of $\mathbf{g}$
$\mathbf{F}$	The gradient of $\mathbf{f}$
$\mathbf{C}_{\text{d}}$	Data covariance matrix
$\mathbf{C}_{\text{geo}}$	Prior covariance matrix for the lithological model parameters
$\mathbf{C}_{\text{phys\|geo}}$	Prior covariance matrix for the physical model parameters conditioned by the lithological model parameters
$\mathbf{C}_{\text{m}}$	Joint prior model covariance matrix
$\mathbf{I}$	Identity matrix
$\mathbf{0}$	Null matrix
∇	Gradient operator
$\mathbf{H}$	Hessian operator
$\Delta\,\mathbf{m}$	The estimated model update for iteration $n+1$

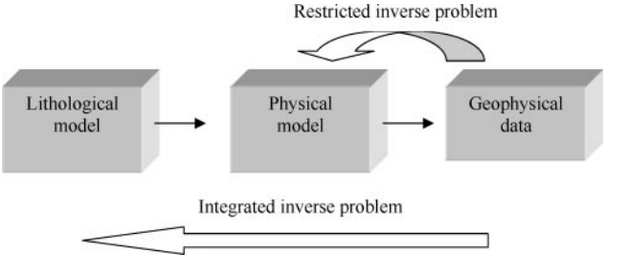

Figure 1. Scheme of the information components in this formulation and comparison with the inverse problem restricted to physical property description. Parameter spaces are shown with boxes, and black arrows indicate links between spaces in the forward direction.

the case in which lithology is described with categories (types of rocks), where a definition of distance is not straightforward. I will use throughout a quadratic norm in data and model parameter spaces for the definition of the factors in the posterior density (expression 2). In the lithological model space, this norm is $\|\mathbf{m}_{\text{geo}}\|^2 = \mathbf{m}_{\text{geo}}{}^{\text{t}}\mathbf{C}_{\text{geo}}^{-1}\mathbf{m}_{\text{geo}}$, with $\mathbf{C}_{\text{geo}}$ an appropriate covariance matrix describing variability and correlation between lithological parameters. Using this norm and the distance from a prior most probable model, prior probabilities are defined in the lithological model space with the multivariate Gaussian density

$$\rho_{\text{geo}}(\mathbf{m}_{\text{geo}}) = c_1 \exp[-{}^1\!/_2(\mathbf{m}_{\text{geo}} - \mathbf{m}_{\text{geo prior}})^{\text{t}}\mathbf{C}_{\text{geo}}{}^{-1} \times (\mathbf{m}_{\text{geo}} - \mathbf{m}_{\text{geo prior}})], \quad (3)$$

with c_1 an appropriate normalization constant. Normalization constants will be implied afterwards because they are relevant to the solution to be derived below.

I define the norm in the data space by $\|\mathbf{d}\|^2 = \mathbf{d}^{\text{t}}\mathbf{C}_{\text{d}}^{-1}\mathbf{d}$ with $\mathbf{C}_{\text{d}}$ being the data covariance matrix that describes second-order statistics on the data uncertainties. To describe the likelihood of the physical property field according to the distance between calculated and observed data, I use the function

$$L(\mathbf{m}_{\text{phys}}) = \exp[-{}^1\!/_2(\mathbf{g}(\mathbf{m}_{\text{phys}}) - \mathbf{d}_{\text{obs}})^{\text{t}} \times \mathbf{C}_{\text{d}}^{-1}(\mathbf{g}(\mathbf{m}_{\text{phys}}) - \mathbf{d}_{\text{obs}})], \quad (4)$$

with $\mathbf{g} : \mathbf{m}_{\text{phys}} \rightarrow \mathbf{d}$, being the function solving the geophysical forward problem, $\mathbf{d}_{\text{cal}} = \mathbf{g}(\mathbf{m}_{\text{phys}})$.

The most interesting factor of the posterior density, expression 2, is the conditional density term because it incorporates the dependency between physical medium properties and the lithological description of the medium, which I describe with a Gaussian model. I consider a function, $\mathbf{f} : \mathbf{m}_{\text{geo}} \rightarrow \mathbf{m}_{\text{phys}}$, to describe the centroid of the distribution, and the matrix $\mathbf{C}_{\text{phys|geo}}$ to describe covariances of the deviations from the centroid:

$$\pi(\mathbf{m}_{\text{phys}}|\mathbf{m}_{\text{geo}}) = c_2 \exp[-{}^1\!/_2(\mathbf{m}_{\text{phys}} - \mathbf{f}(\mathbf{m}_{\text{geo}}))^{\text{t}} \times \mathbf{C}_{\text{phys|geo}}^{-1}(\mathbf{m}_{\text{phys}} - \mathbf{f}(\mathbf{m}_{\text{geo}}))], \quad (5)$$

with the corresponding norm defined by $\|\mathbf{m}_{\text{phys}}\|^2 = \mathbf{m}_{\text{phys}}^{\text{t}}\mathbf{C}_{\text{phys|geo}}^{-1}\mathbf{m}_{\text{phys}}$.

By inserting each one of the factors above in the posterior density (expression 2), the later is given by $\sigma(\mathbf{m}_{\text{phys}}, \mathbf{m}_{\text{geo}}) = c \exp[-S]$, with the half-sum of squares S being

$$S = {}^1\!/_2 \underbrace{(\mathbf{g}(\mathbf{m}_{\text{phys}}) - \mathbf{d}_{\text{obs}})^{\text{t}}\mathbf{C}_{\text{d}}^{-1}(\mathbf{g}(\mathbf{m}_{\text{phys}}) - \mathbf{d}_{\text{obs}})}_{\text{geophysics}} + {}^1\!/_2 \underbrace{(\mathbf{m}_{\text{phys}} - \mathbf{f}(\mathbf{m}_{\text{geo}}))^{\text{t}}\mathbf{C}_{\text{phys|geo}}^{-1}(\mathbf{m}_{\text{phys}} - \mathbf{f}(\mathbf{m}_{\text{geo}}))}_{\text{petrophysics}} + {}^1\!/_2 \underbrace{(\mathbf{m}_{\text{geo}} - \mathbf{m}_{\text{geo prior}})^{\text{t}}\mathbf{C}_{\text{geo}}^{-1}(\mathbf{m}_{\text{geo}} - \mathbf{m}_{\text{geo prior}})}_{\text{geology}}. \quad (6)$$

Notice that the inverse covariance matrices weight the contribution of each type of information to the total sum of squares. Above, $\mathbf{g}(\mathbf{m}_{\text{phys}})$ and $\mathbf{f}(\mathbf{m}_{\text{geo}})$, are nonlinear functions that incorporate complexity on the shape of the posterior density. The posterior density is not a Gaussian function due to this nonlinearity. The functions $\mathbf{g}(\mathbf{m}_{\text{phys}})$ and $\mathbf{f}(\mathbf{m}_{\text{geo}})$ are here considered well behaved enough to have derivatives.

In many cases, parameters describing lithology, like porosity and composition, are positive and lognormally distributed, instead of normally distributed. If the parameters are strongly constrained or far from the origin, the difference between the two probability densities may not be relevant. But in cases where the variability is large or the parameters are evaluated near the origin, the difference is significant, and the lognormal model should be used. To comply with a lognormal distribution, the actual model lithological parameters $\mathbf{m}_{\text{geo}}$ should be the logarithm of the property (composition, porosity, etc.). The same comment is valid for the parameters describing the physical media properties $\mathbf{m}_{\text{phys}}$, if their distribution is lognormal.

Figure 2 shows the type of relationship exploited in this formulation, linking physical media behavior to rock properties in earth media. The figure shows examples of statistical relationship between lithological and physical properties for a general case (Figure 2a), the relation between mass density and silica weight content in crustal rocks based on the work by Christensen and Mooney (1995)(Figure 2b), and the relation between compressional velocity and porosity in sandstones based in data from Han et al. (1986)(Figure 2c). Figure 2 refers to overall behavior of the property. Actual property fields are defined in space and comply not only with overall relations as shown by Figure 2, but with relations describing the spatial continuity as well. This is described in the nondiagonal terms of the matrices $\mathbf{C}_{\text{phys|geo}}$and $\mathbf{C}_{\text{geo}}$ to be defined with the appropriate covariance functions [see Isaaks and Srivastava (1989) for a review of covariance function models].

SOLUTION BY OPTIMIZATION

The terms in the objective function (expression 6) demand proximity between the calculated and observed data, proximity of physical media properties with the corresponding expectations according to media lithology, and proximity of the lithology with the prior lithological model. Minimizing the objective function (maximizing the posterior density) achieves the goal of finding models that jointly explain geophysical, petrophysical, and geological information. I use the gradient and the Hessian of the objective function in the optimization algorithm to iteratively approach a model that maximizes the posterior probability density.

Taking partial derivatives of the objective function, we end up with the formulas for the gradients (Appendix A) ,

$$\nabla_{\text{geo}} S = \mathbf{C}_{\text{geo}}^{-1}(\mathbf{m}_{\text{geo}} - \mathbf{m}_{\text{geo prior}}) - \mathbf{F}^{\text{t}}\mathbf{C}_{\text{phys|geo}}^{-1}(\mathbf{m}_{\text{phys}} - \mathbf{f}(\mathbf{m}_{\text{geo}})), \quad (7)$$

$$\nabla_{\text{phys}} S = \mathbf{C}_{\text{phys|geo}}^{-1}(\mathbf{m}_{\text{phys}} - \mathbf{f}(\mathbf{m}_{\text{geo}})) + \mathbf{G}^{\text{t}}\mathbf{C}_{\text{d}}^{-1}(\mathbf{g}(\mathbf{m}_{\text{phys}}) - \mathbf{d}_{\text{obs}}). \quad (8)$$

In expressions 7 and 8; $\mathbf{G} = (\partial\mathbf{g}/\partial\mathbf{m}_{\text{phys}})$ and $\mathbf{F} = (\partial\mathbf{f}/\partial\mathbf{m}_{\text{geo}})$ are the gradient of $\mathbf{g}(\mathbf{m}_{\text{phys}})$ and $\mathbf{f}(\mathbf{m}_{\text{geo}})$ correspondingly. The ∇_{geo} and ∇_{phys} operators represent differentiation respect to the lithological model parameters $(\partial/\partial\mathbf{m}_{\text{geo}})$ and the physical model parameters $(\partial/\partial\mathbf{m}_{\text{phys}})$, correspondingly.

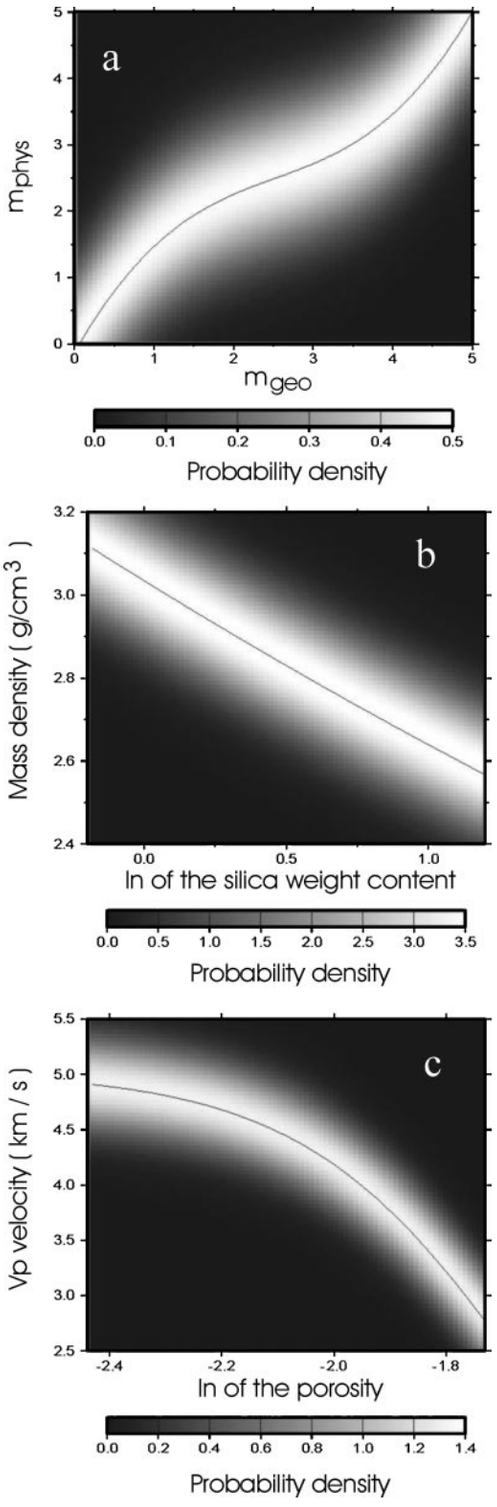

Figure 2. Examples of information linking lithological and physical media properties for (a) a general case, (b) dependency of the mass density with the logarithm of the silica weight content, and (c) dependency of the compressional velocity with the logarithm of the porosity in sandstones. Gray tones indicate values of the conditional probability density, and the solid line represents the center of the conditional density [the function $\mathbf{f}(\mathbf{m}_{\text{geo}})$].

I obtain the Hessian of the objective function by differentiating again (Appendix A). Another important component required for the optimization is the covariance matrix in the joint model space, which is obtained from $\mathbf{C}_{\text{geo}}^{-1}$, $\mathbf{C}_{\text{phys|geo}}^{-1}$, and $\mathbf{F}$ defined above (see Appendix A). Below, I derive expressions for a common optimization approach: Newton's method. Other common approaches can be set up from these basic formulas with appropriate modification.

The normal equations (Newton's method)

At minimal values of the objective function, the gradient is null. This condition is used to obtain the normal equations for the lithological inversion problem. By expanding the gradient of S, $\nabla S[\mathbf{m}_{n+1}] \approx \mathbf{H}(S)[\mathbf{m}_n]\Delta\mathbf{m} + \nabla S[\mathbf{m}_n]$, and equating the left term to zero, the set of normal equations, $\mathbf{H}(S)[\mathbf{m}_n]\Delta\mathbf{m} = -\nabla S[\mathbf{m}_n]$, are obtained. In the latter expression, $\Delta\mathbf{m}$ is the estimated step in the model space, $\Delta\mathbf{m} = \mathbf{m}_{n+1} - \mathbf{m}_n$, in order to minimize the function S, $\mathbf{H}(S)[\mathbf{m}_n]$ is the Hessian of S evaluated at the current model, and $\nabla S[\mathbf{m}_n]$ the gradient of S evaluated at the current model. Solving $\Delta\mathbf{m}$ in the linear system of equations produces the model update.

I left multiply the normal equations by the model covariance matrix, producing the equations

$$\underbrace{\mathbf{C}_m\mathbf{H}(S)[\mathbf{m}_n]}_{\text{curvature}}\Delta\mathbf{m} = \underbrace{-\mathbf{C}_m\nabla S[\mathbf{m}_n]}_{\text{steepest descent direction}}, \qquad (9)$$

where the left matrix is the curvature of the objective function, and the right term is the direction of steepest descent. After inserting in the curvature term the expressions for the Hessian and the joint covariance matrix (Appendix A), the system takes the following triangular structure:

$$\begin{pmatrix} \mathbf{I} & \mathbf{C}_{\text{geo}}\mathbf{F}^t\mathbf{G}^t\mathbf{C}_d^{-1}\mathbf{G} \\ \mathbf{0} & \mathbf{I} + (\mathbf{C}_{\text{phys|geo}} + \mathbf{F}\mathbf{C}_{\text{geo}}\mathbf{F}^t)\mathbf{G}^t\mathbf{C}_d^{-1}\mathbf{G} \end{pmatrix} \begin{pmatrix} \Delta\mathbf{m}_{\text{geo}} \\ \Delta\mathbf{m}_{\text{phys}} \end{pmatrix} = -\mathbf{C}_m\nabla S. \qquad (10)$$

The size of the joint linear system in the normal equations is reduced to two smaller linear systems, which is convenient for solving the system of equations. The second line of equation 10 provides calculation of $\Delta\mathbf{m}_{\text{phys}}$, which can be used then to solve for $\Delta\mathbf{m}_{\text{geo}}$with the linear equations of the first line. Making the substitutions for the right side with the expression for the steepest descent direction (Appendix A) and the joint model covariance, the model update for the physical model parameters gives $\mathbf{A}\Delta\mathbf{m}_{\text{phys}} = \mathbf{b}$, with

$$\mathbf{A} = \mathbf{I} + (\mathbf{C}_{\text{phys|geo}} + \mathbf{F}\mathbf{C}_{\text{geo}}\mathbf{F}^t)\mathbf{G}^t\mathbf{C}_d^{-1}\mathbf{G}, \qquad (11)$$

and $\mathbf{b} = \mathbf{f}(\mathbf{m}_{\text{geo}}) - \mathbf{m}_{\text{phys}}^n + \mathbf{F}(\mathbf{m}_{\text{geo prior}} - \mathbf{m}_{\text{geo}}) + (\mathbf{C}_{\text{phys|geo}} + \mathbf{F}\mathbf{C}_{\text{geo}}\mathbf{F}^t)\mathbf{G}^t\mathbf{C}_d^{-1}(\mathbf{d}_{\text{obs}} - \mathbf{g}(\mathbf{m}_{\text{phys}}^n))$.

This linear system of equations can be solved by conventional algorithms (e.g., Gauss-Newton triangularization method, biconjugated gradients). For the selection of the method, it should be taken into account that the left matrix is in general not symmetric. Notice that the dimensions of this system are the same as for a conventional inversion (hence, computations are not significantly larger), although the formulation incorporates information about the dependency between lithology

and physical media properties, and the statistics of the physical and lithological properties.

For the update in the lithological model space, the equation obtained from the first line of the joint linear system, (expression 10) is

$$\Delta\mathbf{m}_{\text{geo}} = \mathbf{m}_{\text{geo prior}} - \mathbf{m}^{\text{n}}_{\text{geo}} + \mathbf{C}_{\text{geo}}\mathbf{F}^{\text{t}}\mathbf{G}^{\text{t}}\mathbf{C}_{\text{d}}^{-1}\left(\mathbf{d}_{\text{obs}} - \mathbf{g}\left(\mathbf{m}^{\text{n}}_{\text{phys}}\right) - \mathbf{G}\Delta\mathbf{m}_{\text{phys}}\right). \quad (12)$$

Expressions 11 and 12 provide the model update for an iteration in the optimization. As it is a nonlinear problem $\mathbf{g}(\mathbf{m}^{\text{n}}_{\text{phys}})$, $\mathbf{G}$ and $\mathbf{F}$ are dependent on the iteration. The iterative procedure can be summarized as follows:

1) Calculate $\mathbf{g}(\mathbf{m}^{\text{n}}_{\text{phys}})$, $\mathbf{f}(\mathbf{m}^{\text{n}}_{\text{geo}})$, $\mathbf{G}$ and $\mathbf{F}$ for the current model n.
2) Solve the system of equations for the physical model update (expression 11).
3) Calculate the lithological mode update (formula 12).
4) Update the lithological and physical model and return to step 1.

Repeat until convergence in reduction of the objective function (expression 6).

COMPARISON WITH NONLITHOLOGICAL INVERSION

Expressions for the lithological inversion presented in the previous subsections agree with the formulation restricted to the physical dimensions of the model, with certain simplifications. A comparison can be made between the physical component of the model update in the inversion approach here developed and the correspondent model update for the inversion based exclusively on physical information. The normal equations for the latter problem can be obtained with the general formula (Tarantola, 1987)

$$(\mathbf{I} + \mathbf{C}_{\text{phys}}\mathbf{G}^{\text{t}}\mathbf{C}_{\text{d}}^{-1}\mathbf{G})\Delta\mathbf{m}_{\text{phys}} = \mathbf{m}_{\text{phys prior}} - \mathbf{m}^{\text{n}}_{\text{phys}} + \mathbf{C}_{\text{phys}}\mathbf{G}^{\text{t}}\mathbf{C}_{\text{d}}^{-1}(\mathbf{d}_{\text{obs}} - \mathbf{g}(\mathbf{m}^{\text{n}}_{\text{phys}})), \quad (13)$$

with the model parameters describing the physical property field.

This formula is equivalent to the formula obtained here for the physical model update (expression 11) after simplification with the following three assumptions:

1) The dependency between physical and lithological properties, described by $\mathbf{f}(\mathbf{m}_{\text{geo}})$, is linear.
2) The prior physical property model is the image of the prior lithological model by the $\mathbf{m}_{\text{phys prior}} = \mathbf{f}(\mathbf{m}_{\text{geo prior}})$.
3) The model covariance matrix above is taken as

$$\mathbf{C}_{\text{phys}} = \mathbf{C}_{\text{phys|geo}} + \mathbf{F}\mathbf{C}_{\text{geo}}\mathbf{F}^{\text{t}}. \quad (14)$$

The third condition on the covariance matrix is to be expected as it is shown in Appendix A that the matrix is the marginal in the physical model space of the joint covariance matrix for the lithological inversion formulation.

It is important to highlight that because the dependency between lithology and physical properties is in general nonlinear, the gradient of the lithology-physical property transform (matrix $\mathbf{F}$), depends on the current model, $\mathbf{m}_{\text{geo}}$. Hence, $\mathbf{C}_{\text{phys}}$ would be actually variable throughout the inversion. This dependency is not taken into account in a conventional formulation restricted to physical parameter space, in which $\mathbf{C}_{\text{phys}}$ is not iteration dependent.

NUMERICAL EXAMPLE OF POROSITY PREDICTION FROM SEISMIC AMPLITUDES

I illustrate the lithological inversion methodology with a synthetic example of joint porosity-impedance estimation from zero-offset reflection seismic data. The earth model is 1D, horizontally layered, with layers of constant impedance and porosity. Seismic data and the earth model are both described in two-way traveltime. The seismic data are simulated by convolving a source function with the reflectivity series calculated from the impedance model, taking into account amplitude changes due to transmisivity. For simplicity, neither multiple reflections nor attenuation are not included in these calculations.

I use Wyllie's formula (Wyllie et al., 1956) to construct the statistical relationship between impedance and porosity in these tests. With the product of Wyllie's transforms for density and P-wave velocity,

$$Z(\phi) = V_{\text{matrix}}\,\rho_{\text{matrix}}[1 - \phi(1 - \rho_{\text{fluid}}/\rho_{\text{matrix}})]/[1 - \phi(1 - V_{\text{matrix}}/V_{\text{fluid}})], \quad (15)$$

where Z is the impedance; ϕ is the porosity defined as the ratio of pore volume to total volume; and, ρ_{fluid} , ρ_{matrix} , V_{fluid}, and V_{matrix} are the mass densities and P-wave velocities for the rock fluid and matrix. This choice of transform is not intrinsic to the method, a formula that suits impedance-porosity data from the particular study area could be used in its place.

Conventional porosity, as in equation 15, is not a convenient parameter for model simulation and least-squares inversion. It is not Gaussian distributed because it is restricted to values from zero to one. I use here an appropriate transformation of the porosity as parameter for definition of probability densities, simulation, and inversion: the logarithm of the ratio between pore volume and matrix volume. However, for most plots and results, I show conventional porosity for easier interpretation.

This logarithmic porosity is related to conventional porosity by $\phi^* = ln[\phi/(1-\phi)]$, or, inversely, $\phi = \exp[\phi^*]/(1+\exp[\phi^*])$. Hence, Wyllie's transform of the logarithmic porosity is

$$Z(\phi^*) = V_{\text{matrix}}\,\rho_{\text{matrix}}(1 + \exp[\phi^*]\rho_{\text{fluid}}/\rho_{\text{matrix}})/(1 + \exp[\phi^*]V_{\text{matrix}}/V_{\text{fluid}}). \quad (16)$$

With this parameterization, the geological model parameters are the logarithmic porosities for the successive horizontal layers, $\mathbf{m}_{\text{geo}} = (\phi^*_1, \phi^*_2, \ldots, \phi^*_{\text{N}})$, and the physical model parameters are the corresponding layer impedances, $\mathbf{m}_{\text{phys}} = (Z_1, Z_2, \ldots, Z_{\text{N}})$. The function that relates the geological parameters to the prior mean physical parameters is $\mathbf{f}(\mathbf{m}_{\text{geo}}) = (Z(\phi^*_1), Z(\phi^*_2), \ldots, Z(\phi^*_N))$, Wyllie's transform of the logarithmic porosity.

I complete the prior statistical model defining covariance matrices, $\mathbf{C}_{\text{geo}}$ and $\mathbf{C}_{\text{phys|geo}}$, which describe the deviations from the mean and the time correlation for logarithmic porosity and impedance, respectively. Both logarithmic porosity and impedances are time related in these tests, following a Gaussian covariance function. For the following tests, I use a covariance

time range of 40 ms for porosity and impedance deviations, and a standard deviation of 5×10^5 Kg s^{-1}m^{-2} for the impedance deviation from the Wyllie's transform of the porosity. The range of porosities and impedances in the models vary in the tests (as will be shown) in order to consider two types of ranges: (1) the nonlinear part of the petrophysical transform, and (2) an almost linear part of the petrophysical transform. I use common values for matrix and fluid parameters of the Wyllie's transform 5600 m/s, 1587 m/s, 2600 kg/m^3, and 1000 kg/m^3 for V_{matrix}, V_{fluid}, ρ_{matrix}, and ρ_{fluid} ,respectively (Hilterman, 2001).

The "true" porosity model in Figure 3 shows a porosity time series generated from the prior statistical model (expression 2) using a conventional multivariate Gaussian simulation technique. The porosity series is transformed to impedance using Wyllie's formula, and then multivariate Gaussian deviations are added (expression 5). The zero-offset seismic reflection amplitudes are calculated from the impedance model with the convolutional process. This simulated porosity-impedance profile and the corresponding simulated seismic zero-offset trace are regarded as the "true" medium parameters and seismic data for testing the inversion technique. Figure 4 shows the porosity-impedance crossplots corresponding to the "true" model shown in Figure 3, superposed on the Wyllie's transform. Layer porosities and impedances are distributed on the nonlinear range of the petrophysical transform.

I perform calculations for the lithological inversion (i.e., the joint porosity-impedance inversion) using Newton's method (expressions 11–12). Matrix **F**, composed of derivatives of the impedance with respect to logarithmic porosity, is obtained by differentiating expression 16. Matrix **G** is the Frechet's derivatives through the reflectivity-transmisivity calculation from impedances and the convolution with the source. Also, I implement a conventional two-step inversion procedure for comparison. This consists of nonlithological least-squares inversion of impedance using Newton's method (expression 13), followed with the inverse of the petrophysical transform to map the estimated impedance model to porosity. Prior information on the impedance is defined to meet the equivalency criteria discussed in the previous section: using the marginal covariance of the impedance (expression 14) and taking the impedance prior mean value from the Wyllie's transform of the porosity prior mean value.

Figure 3 shows the results of the joint and two-step inversions for the data corresponding to the "true" model. The joint inversion is significantly closer to the "true" porosity and impedance model than the two-step inversion. Figure 5 shows crossplots of predicted and "true" values of porosity and impedance, indicating better prediction for the lithological inversion technique than for the conventional step-wise technique. I use two quantitative criteria for comparing fitness to the targeted ("true") model: the correlation of the predicted-estimated crossplots and the rms error. With both indicators, the joint lithological inversion performed better.

Keeping the same type of statistical parameters and porosity ranges, but using different random number sequences, 20 independent porosity-impedance simulations were generated and the corresponding zero-offset seismic trace inverted. Lithological joint inversion systematically performed better than the

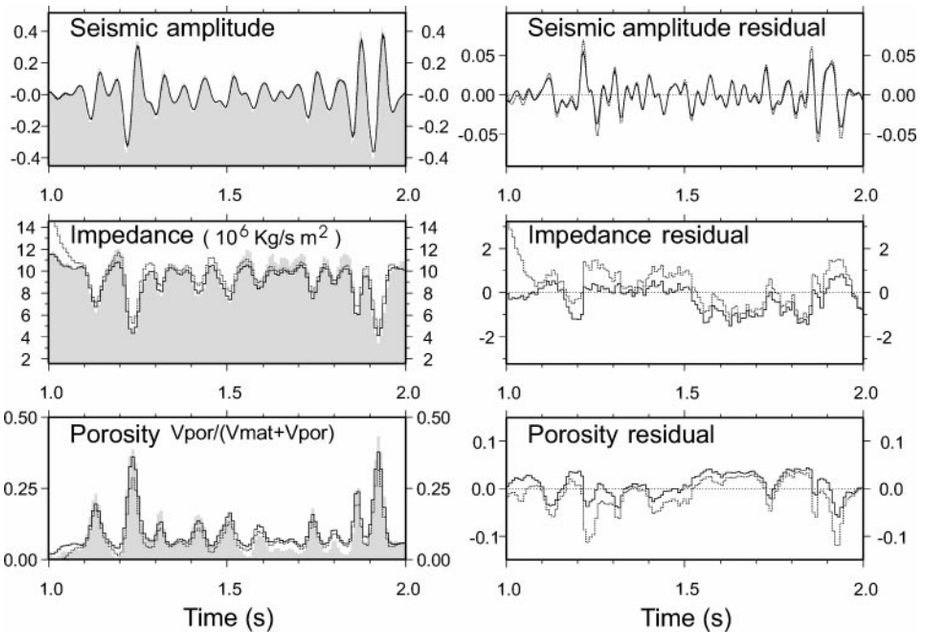

Figure 3. Inversion test showing a "true" porosity-impedance model and the corresponding seismic data (gray sections), the porosity and impedance estimated with the lithological inversion and the corresponding seismic data (continuous lines), and the porosity and impedance estimated with the two-step inversion and the corresponding seismic data (dashed lines). Differences between "true" and estimated parameters are shown at the bottom for the lithological (continuous lines) and the two-step inversion (dashed lines). Vpor = pore volume; Vmat = matrix volume.

two-step inversion for all 20 cases. Table 2 summarizes results for the case shown in Figure 3 and average results for the 20 independent cases.

Figure 5 shows another advantage of using lithological inversion. Lithological inversion guarentees that predicted porosities are always positive, whereas the conventional step-wise procedure usually estimate some low porosity values as negative porosities. Negative values for porosity occur in many of the 20 independent cases inverted with the two-step procedure.

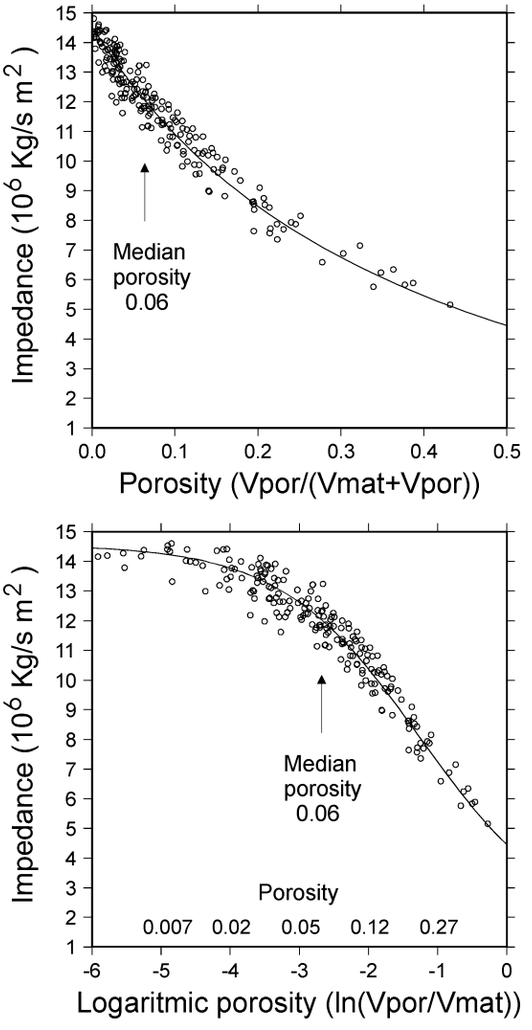

Figure 4. Layer impedance-logarithmic porosity and impedance-porosity crossplots corresponding to the "true" model shown in Figure 3. The line shows the Wyllie's petrophysical transform. Model parameters span on a non-linear part of the petrophysical transform from logarithmic porosity to impedance. Vpor = pore volume; Vmat = matrix volume.

The "true" model in Figure 6 shows a porosity-impedance simulation with a different porosity range and median porosity, all other statistical parameters are the same as for the "true" model shown in Figure 3. Figure 7 shows the porosity-impedance crossplots of the "true" model. In this case, layer parameters are distributed on the linear part of the petrophysical transform with absence of low porosities (below 0.05). In this situation, the improvement of the lithological inversion is not significant compared with the conventional step-wise inversion; both methods are equivalent. This is shown in Figure 6, where the porosity and impedance profiles estimated with the joint and two-step inversion are superposed in most parts. Table 3 shows similar results on correlation between predicted and true parameters, and the rms prediction error.

DISCUSSION

In this work, both in theory and numerical tests, I assume simplifications that are substantial to least-squares optimization. Basically, I consider monomodality of the probability density of physical property parameter conditioned by the lithological parameters, and Gaussian deviations for data errors, physical property deviates from the petrophysical transform, and lithological deviates from the prior model. Quasi-linear behavior of the geophysical forward function and the petrophysical transform [$\mathbf{g}(\mathbf{m})$ and $\mathbf{f}(\mathbf{m})$ in formulas of previous sections] is also an assumption. These assumptions are significant; nevertheless, least-squares optimization is a useful tool that works in many situations. Gaussianity of deviates can be corrected to some point with convenient transforms. However, multimodality is a more difficult problem for optimization techniques. Monte Carlo methods provide general solution to inverse problems without requiring the assumptions of least-squares optimization. See Bosch (1999) and Bosch et al. (2001) for discussion on Monte Carlo implementation of lithological inversion.

Another aspect important to mention is that lithological inversion provides a method for jointly inverting multiple geophysical data sets (Bosch, 1999; Bosch et al., 2001) such as seismic, electrical, gravity, etc. The reason is that the same lithological parameters can be related to several physical rock properties (e.g., impedance, resistivity, density, etc.) providing the required coupling for the multiple data inversion. Because of the statistical links across multiple physical properties and lithology, different geophysical data contribute with complementary information towards the same lithological model parameters. The equations for the least-squares multiple data lithological inversion are the same as in this work with appropriate partitioning of data and model spaces.

Table 2. Prediction rms error and correlation between predicted and "true" values for cases at the nonlinear range of the petrophysical transform.

Description	Joint inversion (case in Figure 3)	Two-step inversion (case in Figure 3)	Joint inversion (20 cases average)	Two-step inversion (20 cases average)
Predicted-true porosity correlation	0.94	0.90	0.94	0.90
Predicted-true impedance correlation	0.92	0.83	0.92	0.82
Porosity prediction rms error	0.032	0.043	0.038	0.048
Impedance prediction rms error (Kg / m s^2)	0.96×10^6	1.19×10^6	1.13×10^6	1.29×10^6

In the numerical examples on porosity prediction from seismic amplitudes, the petrophysical transform I use relating logarithmic porosity and impedance is almost linear for medium to large logarithmic porosities. For this petrophysical transform, results show that if low porosities (below 0.05) are not present in the sequence of layers, a two-step inversion for impedance and porosity is as good as the joint inversion. If low porosities are present in the sequence of layers, the joint inversion provides a better estimation for porosities and impedances than the two-step inversion.

The multiplicity, volume, and quality of information involved in exploration and interpretation progressively increase, creating a technological context in which advanced tomographic techniques are required to jointly exploit geophysical, petrophysical, and geological information. Within the view of model statistical estimation, it is possible to formulate the inverse problem taking into account all the information, extending the concept of geophysical inversion.

Within this approach, it is essential to define a common earth model. It is a model that jointly describes in space physical properties and properties directly related to rock structure and lithology. The convenient lithological description depends on the geology of the area in exploration, targets, and available geophysical techniques. For exploration of sedimentary basins, lithology indicators and porosity are good candidates. In massif areas, silica weight content is a good candidate, grading crustal rocks from basic to acid.

Another aspect of the selection of the lithological property to represent in the model is the influence of the property on the physical behavior of the medium (i.e., the indirect influence in the collected geophysical data). If we want to invert seismic data within this integrated approach, the lithological property described within the model should be statistically related to the elastic parameters. This can be verified in the formula for the lithological model update (expression 12). If there is no correlation between the physical and lithological parameters, the **F** matrix is be zero, producing the trivial estimate $\mathbf{m}_{\text{geo}} = \mathbf{m}_{\text{geo prior}}$. In this case, the geophysical data does not add anything to the previous knowledge of the lithological property.

In this formulation, the lithological medium description is not limited to a single property, it can be more than one. The lithological parameters can be, for example, a combination of a lithology indicator and porosity, $\mathbf{m}_{\text{geo}} = \{\mathbf{m}_{\text{lit}}, \mathbf{m}_{\text{por}}\}$, depending on the available information and the specific targets.

Table 3. Prediction rms error and correlation between predicted and "true" values for cases at the linear range of the petrophysical transform.

Description	Joint inversion (case in Figure 6)	Two-step inversion (case in Figure 6)	Joint inversion (20 cases average)	Two-step inversion (20 cases average)
Predicted-true porosity correlation	0.86	0.85	0.80	0.80
Predicted-true impedance correlation	0.87	0.85	0.79	0.77
Porosity prediction rms error	0.040	0.039	0.048	0.048
Impedance prediction rms error (Kg/m s^2)	0.88×10^6	0.87×10^6	1.08×10^6	1.08×10^6

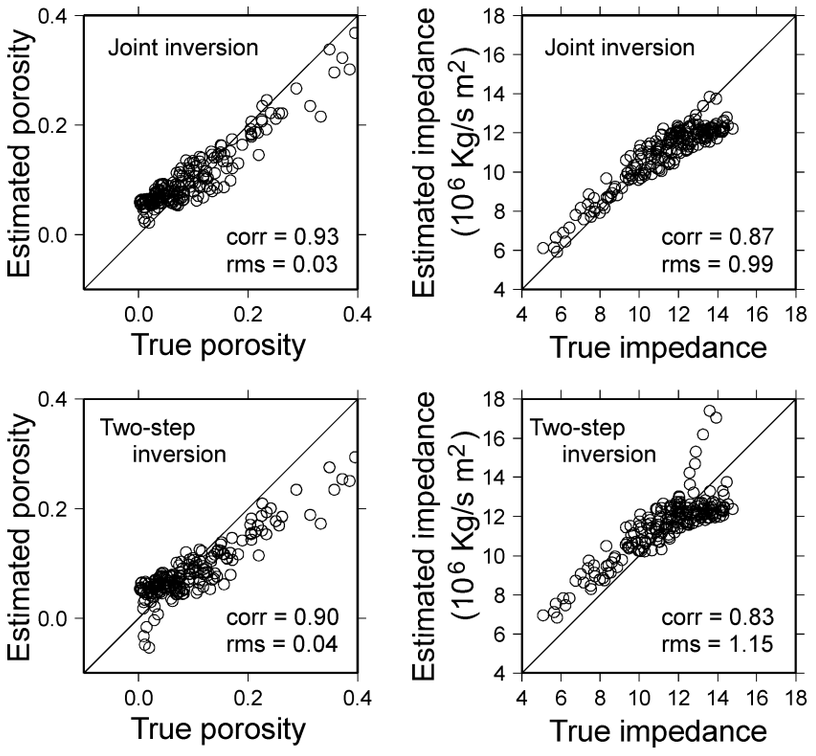

Figure 5. Crossplots comparing "true" with estimated layer parameters corresponding to the porosity-impedance models shown in Figure 3, obtained with the lithological and nonlithological formulation using Newton's method.

CONCLUSIONS

Using the approach of lithological inversion, I extend least-squares optimization techniques commonly used in geophysical inversion to produce joint estimation of lithology and physical media properties . The principle is to optimize a composed earth model that jointly describes media physics and lithology in order to explain geophysical observations and fit geostatistical relations between physical media properties and lithology. The model updates comprehend modifications to the physical property field and the lithological property field.

The formulation considers nonlinear dependence of the calculated geophysical data from physical media properties, and nonlinear dependence of the expected physical media properties from lithology media properties. I present the solution to model updates, following iterative linearization of the problem, for the common Newton's optimization method. From this method, extension to others can be done.

The results obtained in this work show that lithological least-squares inversion performs better in predicting both geological parameters and physical parameters than the conventional two-step inversion approach. The latter consists of least-squares inversion to estimate the physical medium parameters followed by the petrophysical inverse transform. When the petrophysical transform is linear the two approaches are equivalent, as shown both in theory and synthetic tests.

ACKNOWLEDGMENTS

Thanks to Yonghe Sun (assistant editor), Wenying Cai (associate editor), Albert Tarantola (IPGP), and an anonymous referee for their constructive reviews. During the major part of this work, the author was a visiting fellow at the Department of Earth Sciences, University of Cambridge.

APPENDIX A

FORMULAS FOR THE GRADIENT, HESSIAN, STEEPEST DESCENT DIRECTION, AND CURVATURE OF THE OBJECTIVE FUNCTION

Gradient of the objective function

The terms in expression 6 of the total sum of squares are noted as $S = S_1 + S_2 + S_3$, with

$$S_1 = {}^1\!/_2 \|\mathbf{g}(\mathbf{m}_{\text{phys}}) - \mathbf{d}_{\text{obs}}\|^2 = {}^1\!/_2 (\mathbf{g}(\mathbf{m}_{\text{phys}}) - \mathbf{d}_{\text{obs}})^{\text{t}} \mathbf{C}_{\text{d}}^{-1} (\mathbf{g}(\mathbf{m}_{\text{phys}}) - \mathbf{d}_{\text{obs}}), \tag{A-1}$$

$$S_2 = {}^1\!/_2 \|\mathbf{m}_{\text{phys}} - \mathbf{f}(\mathbf{m}_{\text{geo}})\|_{\|}^2 = {}^1\!/_2 (\mathbf{m}_{\text{phys}} - \mathbf{f}(\mathbf{m}_{\text{geo}}))^{\text{t}} \mathbf{C}_{\text{phys|geo}}^{-1} (\mathbf{m}_{\text{phys}} - \mathbf{f}(\mathbf{m}_{\text{geo}})), \tag{A-2}$$

$$S_3 = {}^1\!/_2 \|\mathbf{m}_{\text{geo}} - \mathbf{m}_{\text{geo prior}}\|^2 = {}^1\!/_2 (\mathbf{m}_{\text{geo}} - \mathbf{m}_{\text{geo prior}})^{\text{t}} \mathbf{C}_{\text{geo}}^{-1} (\mathbf{m}_{\text{geo}} - \mathbf{m}_{\text{geo prior}}). \tag{A-3}$$

Gradients with respect to physical-property description parameters $\mathbf{m}_{\text{phys}}$ and lithology description parameters $\mathbf{m}_{\text{geo}}$ are,

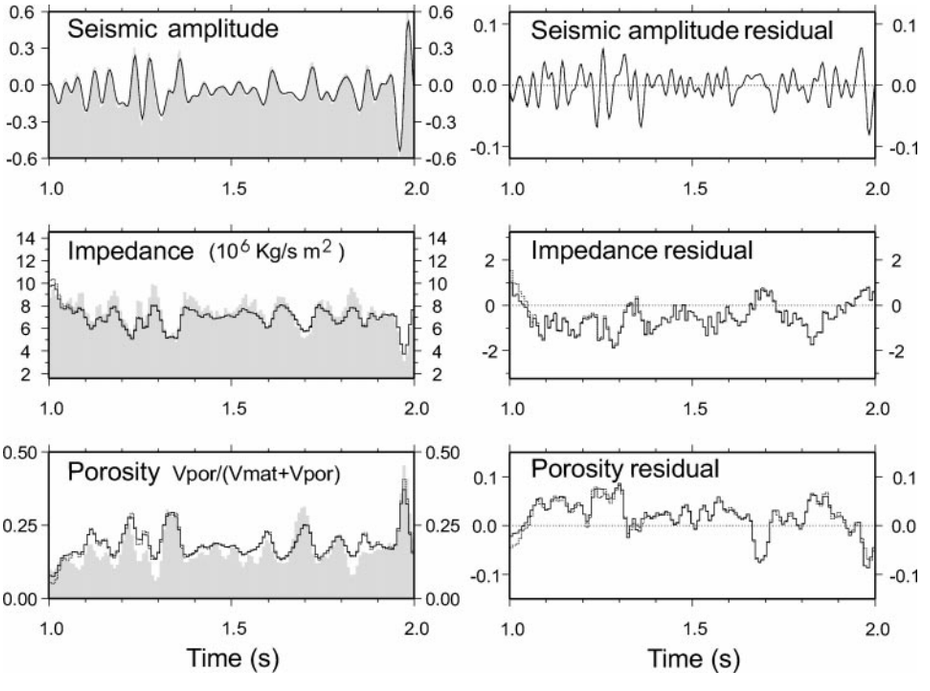

Figure 6. Inversion test showing a "true" porosity-impedance model and corresponding seismic data (gray sections), the porosity and impedance estimated with the lithological inversion and the corresponding seismic data (continuous lines), and the porosity and impedance estimated with the two-step inversion and the seismic corresponding data (dashed lines). Differences between true and estimated parameters are shown at the bottom for the joint (continuous lines) and two-step (dashed lines) inversion.

for each term separately,

$$\begin{aligned}
\nabla_{\text{geo}} S_1 &= 0,\\
\nabla_{\text{phys}} S_1 &= \mathbf{G}^{\text{t}}\mathbf{C}_{\text{d}}^{-1}(\mathbf{g}(\mathbf{m}_{\text{phys}}) - \mathbf{d}_{\text{obs}}),\\
\nabla_{\text{geo}} S_2 &= -\mathbf{F}^{\text{t}}\mathbf{C}_{\text{phys|geo}}^{-1}(\mathbf{m}_{\text{phys}} - \mathbf{f}(\mathbf{m}_{\text{geo}})),\\
\nabla_{\text{phys}} S_2 &= \mathbf{C}_{\text{phys|geo}}^{-1}(\mathbf{m}_{\text{phys}} - \mathbf{f}(\mathbf{m}_{\text{geo}})),\\
\nabla_{\text{geo}} S_3 &= \mathbf{C}_{\text{geo}}^{-1}(\mathbf{m}_{\text{geo}} - \mathbf{m}_{\text{geo prior}}),\\
\nabla_{\text{phys}} S_3 &= 0,
\end{aligned}$$

with $\mathbf{G} = (\partial\mathbf{g}/\partial\mathbf{m}_{\text{phys}})$ and $\mathbf{F} = (\partial\mathbf{h}/\partial\mathbf{m}_{\text{geo}})$ being the gradient of $\mathbf{g}(\mathbf{m}_{\text{phys}})$ and $\mathbf{f}(\mathbf{m}_{\text{geo}})$, respectively. Adding the three terms in the gradient of the objective function gives

$$\begin{aligned}
\nabla_{\text{geo}} S &= \mathbf{C}_{\text{geo}}^{-1}(\mathbf{m}_{\text{geo}} - \mathbf{m}_{\text{geo prior}})\\
&\quad - \mathbf{F}^{\text{t}}\mathbf{C}_{\text{phys|geo}}^{-1}(\mathbf{m}_{\text{phys}} - \mathbf{f}(\mathbf{m}_{\text{geo}})), \qquad \text{(A-4)}\\
\nabla_{\text{phys}} S &= \mathbf{C}_{\text{phys|geo}}^{-1}(\mathbf{m}_{\text{phys}} - \mathbf{f}(\mathbf{m}_{\text{geo}}))\\
&\quad + \mathbf{G}^{\text{t}}\mathbf{C}_{\text{d}}^{-1}(\mathbf{g}(\mathbf{m}_{\text{phys}}) - \mathbf{d}_{\text{obs}}). \qquad \text{(A-5)}
\end{aligned}$$

The complete gradient of S is the combination of equations A-4 and A-5:

$$\nabla S = \begin{pmatrix} \nabla_{\text{geo}} \\ \nabla_{\text{phys}} \end{pmatrix}. \qquad \text{(A-6)}$$

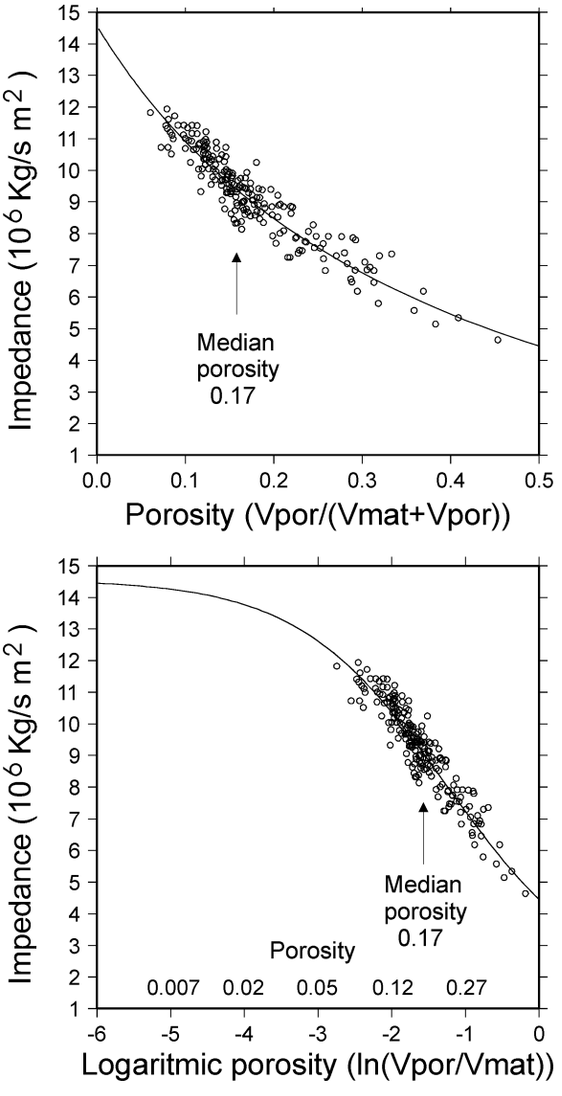

Figure 7. Layer impedance-logarithmic porosity and impedance-porosity crossplots corresponding to the "true" model shown in Figure 6. The line shows the Wyllie's petrophysical transform from logarithmic porosity to impedance, and porosity to impedance. Model parameters span on an almost linear part of the petrophysical transform in this case.

Approximation of the Hessian of the objective function

The Hessian of S is needed for the formulation of the Newton's method of optimization in which it enters into the calculation of the model update and posterior covariance. As usual in Newton's method, I consider that the current point and the updated point in the model space are close enough that linear approximation of functions $\mathbf{f}(\mathbf{m}_{\text{geo}})$ and $\mathbf{g}(\mathbf{m}_{\text{phys}})$ is good, and the second–order terms in the functions expansion can be neglected. Terms in the Hessian of S involving second derivatives of $\mathbf{f}(\mathbf{m}_{\text{geo}})$ and $\mathbf{g}(\mathbf{m}_{\text{phys}})$ are neglected below. This is called a quasi-linear approximation of the Hessian of *S*.

The Hessian is the operator of the second derivatives of S respect to the model parameters:

$$\mathbf{H} = (\partial^2 S/\partial \mathrm{m}^{\mathrm{i}}\partial \mathrm{m}^{\mathrm{j}}) = \begin{pmatrix} \nabla_{\text{geo}}\nabla_{\text{geo}} S & \nabla_{\text{phys}}\nabla_{\text{geo}} S \\ \nabla_{\text{geo}}\nabla_{\text{phys}} S & \nabla_{\text{phys}}\nabla_{\text{phys}} S \end{pmatrix}. \qquad \text{(A-7)}$$

Differentiating the expressions for the gradient, the four components are

$$\begin{aligned}
\nabla_{\text{geo}}\nabla_{\text{geo}} S &= \mathbf{C}_{\text{geo}}^{-1} + \mathbf{F}^{\text{t}}\mathbf{C}_{\text{phys|geo}}^{-1}\mathbf{F}, \qquad \text{(A-8)}\\
\nabla_{\text{phys}}\nabla_{\text{geo}} S &= -\mathbf{F}^{\text{t}}\mathbf{C}_{\text{phys|geo}}^{-1}, \qquad \text{(A-9)}\\
\nabla_{\text{geo}}\nabla_{\text{phys}} S &= -\mathbf{C}_{\text{phys|geo}}^{-1}\mathbf{F}, \qquad \text{(A-10)}\\
\nabla_{\text{phys}}\nabla_{\text{phys}} S &= \mathbf{C}_{\text{phys|geo}}^{-1} + \mathbf{G}^{\text{t}}\mathbf{C}_{\text{d}}^{-1}\mathbf{G}. \qquad \text{(A-11)}
\end{aligned}$$

Model covariance matrix

We previously provided the covariance $\mathbf{C}_{\text{geo}}$ in the lithological model space, and the conditional covariance $\mathbf{C}_{\text{phys|geo}}$. I calculate the covariance in the joint model space in the following way. The probability density in the joint model space is

$$\rho(\mathbf{m}) = \pi(\mathbf{m}_{\text{phys}}|\mathbf{m}_{\text{geo}})\rho_{\text{geo}}(\mathbf{m}_{\text{geo}}). \qquad \text{(A-12)}$$

By substitution of equations 3 and 5, $\rho(\mathbf{m}) = \mathrm{c}_3\exp[S_{\text{prior}}]$, with

$$\begin{aligned}
S_{\text{prior}} &= {}^1\!/_2(\mathbf{m}_{\text{phys}} - \mathbf{f}(\mathbf{m}_{\text{geo}}))^{\text{t}}\mathbf{C}_{\text{phys|geo}}^{-1}(\mathbf{m}_{\text{phys}} - \mathbf{f}(\mathbf{m}_{\text{geo}}))\\
&\quad + {}^1\!/_2(\mathbf{m}_{\text{geo}} - \mathbf{m}_{\text{geo prior}})^{\text{t}}\mathbf{C}_{\text{geo}}^{-1}(\mathbf{m}_{\text{geo}} - \mathbf{m}_{\text{geo prior}}).
\end{aligned} \qquad \text{(A-13)}$$

The joint model inverse covariance matrix $\mathbf{C}_{\text{m}}^{-1}$ is the Hessian of equation A-13, which can be obtained by differentiating two times equation A-13,

$$\mathbf{C}_{\text{m}}^{-1} = \begin{pmatrix} \mathbf{C}_{\text{geo}}^{-1} + \mathbf{F}^{\text{t}}\mathbf{C}_{\text{phys|geo}}^{-1}\mathbf{F} & -\mathbf{F}^{\text{t}}\mathbf{C}_{\text{phys|geo}}^{-1} \\ -\mathbf{C}_{\text{phys|geo}}^{-1}\mathbf{F} & \mathbf{C}_{\text{phys|geo}}^{-1} \end{pmatrix}. \qquad \text{(A-14)}$$

Notice that the only difference between the Hessian of the objective function in the previous section is the data term involving matrices $\mathbf{G}$ and $\mathbf{C}_d$. The joint model covariance is the inverse of equation A-14, given by

$$\mathbf{C}_m = \begin{pmatrix} \mathbf{C}_{geo} & \mathbf{C}_{geo}\mathbf{F}^t \\ \mathbf{F}\mathbf{C}_{geo} & \mathbf{F}\mathbf{C}_{geo}\mathbf{F}^t + \mathbf{C}_{phys|geo} \end{pmatrix}, \qquad \text{(A-15)}$$

which can be verified by making either the right or the left product $\mathbf{C}_m\mathbf{C}_m^{-1} = \mathbf{C}_m^{-1}\mathbf{C}_m = \mathbf{I}$.

Curvature of the objective function

The curvature of the objective function (the matrix in the left term of expression 9) is given by $\mathbf{C}_m\,\mathbf{H}(S)$, factors obtained in previous sections. A quick way to form a compact expression for the product is by expressing the Hessian of S in terms of $\mathbf{C}_m$,

$$\mathbf{H}(S) = \mathbf{C}_m^{-1} + \begin{pmatrix} \mathbf{0} & \mathbf{0} \\ \mathbf{0} & \mathbf{G}^t\mathbf{C}_d^{-1}\mathbf{G} \end{pmatrix}, \qquad \text{(A-16)}$$

as shown in the previous section. Then, the curvature is

$$\begin{aligned} \textbf{Curvature} &= \mathbf{C}_m\mathbf{H}(S) \\ &= \mathbf{I} + \begin{pmatrix} \mathbf{C}_{geo} & \mathbf{C}_{geo}\mathbf{F}^t \\ \mathbf{F}\mathbf{C}_{geo} & \mathbf{F}\mathbf{C}_{geo}\mathbf{F}^t + \mathbf{C}_{phys|geo} \end{pmatrix} \begin{pmatrix} \mathbf{0} & \mathbf{0} \\ \mathbf{0} & \mathbf{G}^t\mathbf{C}_d^{-1}\mathbf{G} \end{pmatrix} \\ &= \begin{pmatrix} \mathbf{I} & \mathbf{C}_{geo}\mathbf{F}^t\mathbf{G}^t\mathbf{C}_d^{-1}\mathbf{G} \\ 0 & \mathbf{I} + (\mathbf{C}_{phys|geo} + \mathbf{F}\mathbf{C}_{geo}\mathbf{F}^t)\mathbf{G}^t\mathbf{C}_d^{-1}\mathbf{G} \end{pmatrix} \end{aligned} \qquad \text{(A-17)}$$

Steepest descent direction

The right side of expression 10 is the steepest descent direction. It is given by $-\mathbf{C}_m\nabla S$, each factor having been obtained in the previous sections:

$$\begin{aligned} \mathbf{d}_{steep} &= -\mathbf{C}_m\nabla S = \mathbf{C}_m(-\nabla S) \\ &= \begin{pmatrix} \mathbf{C}_{geo} & \mathbf{C}_{geo}\mathbf{F}^t \\ \mathbf{F}\mathbf{C}_{geo} & \mathbf{F}\mathbf{C}_{geo}\mathbf{F}^t + \mathbf{C}_{phys|geo} \end{pmatrix} \\ &\begin{pmatrix} \mathbf{C}_{geo}^{-1}(\mathbf{m}_{geo\,prior} - \mathbf{m}_{geo}) - \mathbf{F}^t\mathbf{C}_{phys|geo}^{-1}(\mathbf{f}(\mathbf{m}_{geo}) - \mathbf{m}_{phys}) \\ \mathbf{C}_{phys|geo}^{-1}(\mathbf{f}(\mathbf{m}_{geo}) - \mathbf{m}_{phys}) + \mathbf{G}^t\mathbf{C}_d^{-1}(\mathbf{d}_{obs} - \mathbf{g}(\mathbf{m}_{phys})) \end{pmatrix} \end{aligned} \qquad \text{(A-18)}$$

Taking the product, canceling opposite terms, and regrouping makes the left side of equation A-18

$$\mathbf{d}_{steep} = \begin{pmatrix} \mathbf{m}_{geo\,prior} - \mathbf{m}_{geo} + \mathbf{C}_{geo}\mathbf{F}^t\mathbf{G}^t\mathbf{C}_d^{-1}(\mathbf{d}_{obs} - \mathbf{g}(\mathbf{m}_{phys})) \\ \mathbf{F}(\mathbf{m}_{geo\,prior} - \mathbf{m}_{geo}) + \mathbf{f}(\mathbf{m}_{geo}) - \mathbf{m}_{phys} + (\mathbf{F}\mathbf{C}_{geo}\mathbf{F}^t + \mathbf{C}_{phys|geo})\mathbf{G}^t\mathbf{C}_d^{-1}(\mathbf{d}_{obs} - \mathbf{g}(\mathbf{m}_{phys})) \end{pmatrix}. \qquad \text{(A-19)}$$

Where $\mathbf{f}(\mathbf{m}_{geo})$ is linear, the second line in express A-19 can be further simplified by making the substitution $\mathbf{F}(\mathbf{m}_{geo\,prior} - \mathbf{m}_{geo}) = \mathbf{f}(\mathbf{m}_{geo}) - \mathbf{f}(\mathbf{m}_{geo\,prior})$ and canceling terms:

$$\mathbf{d}_{steep} = \begin{pmatrix} \mathbf{m}_{geo\,prior} - \mathbf{m}_{geo} + \mathbf{C}_{geo}\mathbf{F}^t\mathbf{G}^t\mathbf{C}_d^{-1}(\mathbf{d}_{obs} - \mathbf{g}(\mathbf{m}_{phys})) \\ \mathbf{f}(\mathbf{m}_{geo\,prior}) - \mathbf{m}_{phys} + (\mathbf{F}\mathbf{C}_{geo}\mathbf{F}^t + \mathbf{C}_{phys|geo})\mathbf{G}^t\mathbf{C}_d^{-1}(\mathbf{d}_{obs} - \mathbf{g}(\mathbf{m}_{phys})) \end{pmatrix}. \qquad \text{(A-20)}$$

REFERENCES

Bosch, M., 1999, Lithologic tomography: From plural geophysical data to lithology estimation: Journal of Geophysical Research, **104**, 749–766.

Bosch, M., A. Guillen, and P. Ledru, 2001, Lithologic tomography: An application to geophysical data from the Cadomian belt of northern Brittany, France: Tectonophysics, **331**, 197–227.

Bosch, M., and J. McGaughey, 2001, Joint inversion of gravity and magnetic data under lithologic constraints: The Leading Edge, **20**, 877–881.

Christensen, N. I., and W. E. Mooney, 1995, Seismic velocity structure and composition of the continental crust: A global view: Journal of Geophysical Research, **100**, 9761–9788.

Han, D., A. Nur, and D. Morgan, 1986, Effects of porosity and clay content on wave velocities in sandstones: Geophysics, **11**, 2093–2107.

Hilterman, F. J., 2001, Seismic amplitude interpretation: Geophysical Development Corporation.

Isaaks, E. H., and R. M. Srivastava, 1989, Applied geostatistics: Oxford University Press.

Mosegaard, K., S. Singh, D. Snyder, and H. Wagner, 1997, Monte Carlo analysis of seismic reflections from Moho and the W reflector: Journal of Geophysical Research, **102**, 2969–2981.

Tarantola, A., 1987, Inverse problem theory: Methods for data fitting and model parameter estimation: Elsevier.

Torres-Verdin, C., M. Victoria, G. Merletti, and J. Pendrel, 1999, Trace-based and geostatistical inversion of 3-D seismic data for thin-sand delineation: An application in San Jorge Basin, Argentina: The Leading Edge, **18**, 1070–1077.

Wyllie, M. R. J., A. R. Gregory, and L. W. Gardner, 1956, Elastic wave velocities in heterogeneous and porous media: Geophysics, **21**, 41–70.